

ORIGINAL RESEARCH

Cerebral Microbleed Burdens in Specific Brain Regions Are Associated With Disease Severity of Cerebral Autosomal Dominant Arteriopathy With Subcortical Infarcts and Leukoencephalopathy

Chih-Ping Chung, MD, PhD*; Jiun-Wei Chen, MS*; Feng-Chi Chang, MD; Wei-Chi Li, BS; Yi-Chung Lee, MD, PhD; Li-Fen Chen, PhD†; Yi-Chu Liao , MD, PhD†

BACKGROUND: Cerebral autosomal dominant arteriopathy with subcortical infarcts and leukoencephalopathy, caused by *NOTCH3* mutations, is characterized by recurrent ischemic strokes and progressive cognitive decline. It remains unclear whether cerebral microbleeds (CMBs) can serve as a surrogate marker for disease progression in cerebral autosomal dominant arteriopathy with subcortical infarcts and leukoencephalopathy. We aimed to investigate the CMB burdens in *NOTCH3* mutation carriers at different disease stages and test their associations with cognitive performance.

METHODS AND RESULTS: Forty-nine individuals carrying *NOTCH3* cysteine-altering mutations received brain magnetic resonance imaging with T1-weighted and susceptibility-weighted images. Whole brain images were segmented into 14 regions using Statistical Parametric Mapping and FreeSurfer software, and semiautomatic methods were used to locate and quantify the number and volume of CMBs. In our study participants, the median of CMB counts was 13, with a wide individual variation (range, 0–286). CMBs were most frequently present in thalamus, followed by temporal lobe. In the whole brain, the CMB counts and CMB volume ratios (ie, CMB volume divided by the volume of corresponding brain region) gradually increased as the disease advanced. CMB counts in the thalamus and temporal and frontal lobes increased more rapidly than other brain regions as disease progressed. There were significant associations between Mini-Mental State Examination scores and CMB counts in the frontal lobe, temporal lobe, and pons.

CONCLUSIONS: CMBs may have an influential role in the clinical manifestations of cerebral autosomal dominant arteriopathy with subcortical infarcts and leukoencephalopathy. CMB burdens and their distribution in different brain regions may be capable to serve as a disease marker for monitoring the disease severity of cerebral autosomal dominant arteriopathy with subcortical infarcts and leukoencephalopathy.

Key Words: CADASIL ■ cerebral microbleeds ■ Mini-Mental State Examination ■ *NOTCH3* gene

Cerebral autosomal dominant arteriopathy with subcortical infarcts and leukoencephalopathy (CADASIL), caused by mutations in the *NOTCH3* gene, is the most common hereditary cerebral

small-vessel disease (CSVD) worldwide.¹ Individuals carrying the pathogenic *NOTCH3* mutations would develop recurrent ischemic strokes and progressive cognitive decline along the disease course.¹ There are

Correspondence to: Yi-Chu Liao, MD, PhD, Department of Neurology, Taipei Veterans General Hospital, 201 Shih-Pai Rd, Section 2, Taipei 11217, Taiwan. E-mail: ycliao5@vghtpe.gov.tw and Li-Fen Chen, PhD, Institute of Brain Science, National Yang-Ming University, 155 Li-Nong St, Section 2, Peitou, Taipei, Taiwan. E-mail: lfchen@ym.edu.tw

*Dr Chung and Mr. JW Chen contributed equally to this work.

†Dr LF Chen and Dr Liao contributed equally to this work.

For Sources of Funding and Disclosures, see page 10.

© 2020 The Authors. Published on behalf of the American Heart Association, Inc., by Wiley. This is an open access article under the terms of the Creative Commons Attribution-NonCommercial-NoDerivs License, which permits use and distribution in any medium, provided the original work is properly cited, the use is non-commercial and no modifications or adaptations are made.

JAHA is available at: www.ahajournals.org/journal/jaha

CLINICAL PERSPECTIVE

What Is New?

- Our study reveals that the amount and location of cerebral microbleeds (CMBs) are associated with disease duration and cognitive dysfunction in patients with cerebral autosomal dominant arteriopathy with subcortical infarcts and leukoencephalopathy.
- As the disease progresses, CMBs accumulate gradually in all brain regions, especially with a more rapid increase of CMB counts in the thalamus and temporal and frontal lobes.
- After adjusting the influences of age, sex, and education level, CMB counts in the frontal lobe, temporal lobe, and pons remain significantly related to the Mini-Mental State Examination scores in patients with cerebral autosomal dominant arteriopathy with subcortical infarcts and leukoencephalopathy.

What Are the Clinical Implications?

- In addition to other known imaging markers of cerebral autosomal dominant arteriopathy with subcortical infarcts and leukoencephalopathy, CMB burdens and their distribution features may serve as a biomarker to monitor the disease progression in cerebral autosomal dominant arteriopathy with subcortical infarcts and leukoencephalopathy.
- Computer-assisted image analysis using Statistical Parametric Mapping and FreeSurfer software can facilitate the evaluation of CMB burdens across different brain regions.

Nonstandard Abbreviations and Acronyms

CADASIL	cerebral autosomal dominant arteriopathy with subcortical infarcts and leukoencephalopathy
CMB	cerebral microbleed
CSVD	cerebral small-vessel disease
MMSE	Mini-Mental State Examination
MRI	magnetic resonance imaging
SWI	susceptibility-weighted image
WMH	white matter hyperintensity

3 radiologic hallmarks of CADASIL, including lacunes on T1-weighted images, white matter hyperintensities (WMHs) on T2-weighted images, and cerebral microbleeds (CMBs) on T2*-weighted gradient-echo images or susceptibility-weighted images (SWIs).^{2,3} Lacunes can be used as a marker to reflect the disease

severity of CADASIL because the total volume of lacunar infarcts has been shown to be correlated with cognitive impairment and disability.⁴ Contrarily, the severity of WMHs is not correlated to cognitive dysfunction, despite the fact that WMHs in the subcortical regions and temporal poles are characteristic features of CADASIL.^{4,5}

The clinical significance of CMBs in CADASIL has not been investigated comprehensively. Most studies addressed risk factors associated with increased CMB burdens.^{2,6} Only 2 studies tested the influence of CMBs on cognitive decline in *NOTCH3* mutation carriers, revealing conflicting results.^{4,5} Notably, the presence of CMBs in patients with CADASIL not only increases the risks of intracerebral hemorrhage⁷ but also predicts the occurrence of incident ischemic stroke.⁸ The topographic distribution of CMBs is also an important feature that helps differentiating CSVD of various causes. For example, CMBs caused by hypertensive microvasculopathy usually locate in deep brain regions, and CMBs attributed to cerebral amyloid angiopathy would occur strictly in lobar regions.^{9–11} However, the characteristics of CMB distribution in CADASIL remain obscure.

It is unclear how the amount and topographic patterns of CMBs change across different disease stages of CADASIL. In addition, the influence of CMBs on cognitive dysfunction has never been studied in the context of anatomical distribution. To resolve these issues, we used semiautomatic methods to locate CMBs and measure the amount and volume of CMBs. Besides, we enrolled both *NOTCH3* cysteine-altering mutation carriers at pre-clinical stage and CADASIL patients with different disease durations to delineate the propagation of CMBs during disease progression. The present study aims at (1) demonstrating the CMB burdens in subjects carrying *NOTCH3* mutations with specific emphasis on the topographic patterns, (2) evaluating the associations between CMB burdens and cognitive performance, and (3) testing whether CMB burdens of specific anatomical locations could be a marker to monitor the disease severity in patients with CADASIL.

METHODS

The data that support the findings of this study are available from the corresponding author on reasonable request.

Participants

Study participants were from a prospective cohort recruiting subjects with CSVD at Taipei Veterans General Hospital (Taipei, Taiwan) between April 2015

and December 2019. Individuals fulfilling the following criteria were enrolled for genetic analysis of *NOTCH3* mutations: (1) subjects having marked WMHs, defined as Fazekas grade 2 or 3, on neuroimaging¹² and presenting with lacunar infarctions, transient ischemic attacks, cognitive impairment, psychiatric disorders, or gait disturbance, (2) subjects having marked WMHs on neuroimaging and a family history of ischemic stroke or vascular dementia, or (3) subjects from families known to be affected by CADASIL. Only those harboring a cysteine-altering pathogenic mutation in *NOTCH3* were included in this study. All participants provided written informed consents, and the study protocol was approved by the institutional review boards of Taipei Veterans General Hospital.

Cardiovascular Risk Factors and Cognitive Assessments

A questionnaire was used to collect data from patients or/and their family on the demographic information, years of education, smoking habits, and medical histories, including hypertension, diabetes mellitus, hyperlipidemia, stroke (ischemic stroke or intracerebral hemorrhage), and cognitive impairment. The onset age of stroke or/and cognitive impairment was determined by medical records or questionnaires. Disease duration was defined as the interval between the onset year of subjects' initial presentation (stroke or/and cognitive impairment) and the year of brain magnetic resonance imaging (MRI) examination. Global cognitive performance was assessed by Mini-Mental State Examination (MMSE).¹³ Hypertension was defined as a self-report of current antihypertensive agent use or a measurement of systolic blood pressure ≥ 140 mm Hg or diastolic blood pressure ≥ 90 mm Hg on at least 2 occasions.¹⁴ Diabetes mellitus was defined as a self-report of current glucose-lowering agent use or a measurement of hemoglobin A1c $\geq 6.5\%$.¹⁵ Dyslipidemia was defined as a self-report of statin use or a measurement of total cholesterol ≥ 240 mg/dL.¹⁶

Genetic Analyses

Genomic DNA was extracted from peripheral blood samples. Mutation analyses of exons 2 to 24 of *NOTCH3* were performed by polymerase chain reaction amplification using intronic primers and Sanger sequencing.¹⁷ All amplicons were sequenced for both sense and antisense strands using the Big Dye 3.1 dideoxy terminator method (Applied Biosystems, Foster City, CA) and ABI Prism 3700 Genetic Analyzer (Applied Biosystems). Mutations were identified by aligning the amplicon sequences with the

published human *NOTCH3* cDNA sequence (RefSeq NM_000435.2).

Brain MRI Acquisition

All participants underwent a brain MRI study using a 3-T MRI scanner (Signa, GE Healthcare, Milwaukee, WI). High-resolution T1-weighted structural images were acquired using 3-dimensional magnetization-prepared rapid gradient-echo sequence with the following parameters: repetition time=7.1 ms, echo time=2.7 ms, inversion time=450 ms, flip angle=12°, matrix size=256×256, field of view=256×256 mm², number of slices=236, bandwidth=326 Hz/pixel, and voxel size=1×1×1 mm without interslice gap. SWIs were acquired with the following parameters: repetition time=42.3 ms, echo time=25.4 ms, flip angle=15°, matrix size=320×224, field of view=200×200 mm², 136 to 152 slices, depending on the head size of subjects, bandwidth=244 Hz/pixel, voxel size=0.625×0.893×1.0 mm³ without interslice gap, and acquisition time=9 minutes 13 seconds.

CMB Detection

CMBs were defined as small (diameter ≤ 10 mm), rounded, and well-demarcated hypointense lesions on the SWI.^{18,19} The detection and segmentation of CMBs were performed by 2 trained experts (F.C.C., J.W.C.), who were blind to subjects' clinical data, via a customized graphic user interface developed in MATLAB

Table 1. Demographics of the Study Population

Variable	All Study Patricians (n=49)
Age, mean (SD), y	60.4 (11.7)
Men, n (%)	28 (57.1)
Education, mean (SD), y	11.5 (4.3)
MMSE score, mean (SD), range (IQR)	24.3 (6.6), 5–30 (8)
Hypertension, n (%)	23 (46.9)
Diabetes mellitus, n (%)	6 (12.2)
Dyslipidemia, n (%)	18 (36.7)
Cigarette smoking, n (%)	15 (30.6)
Disease stage, n (%)	
Preclinical stage	10 (20.4)
Symptomatic with duration <5 y	22 (44.9)
Symptomatic with duration ≥ 5 y	17 (34.7)
Clinical manifestations	
Stroke, n (%)	33 (67.3)
Cognitive impairment, n (%)	22 (44.9)
Duration of symptom onset, mean (SD), y	4.6 (3.8)

IQR indicates interquartile range; and MMSE, Mini-Mental State Examination.

Table 2. CMB Burdens in Each Brain Region (All Study Participants, N=49)

Variable	Presence of CMBs, n (%)	CMB Count, Median (Range)	Brain Volume, Median (Range), cm ³	CMB Volume Ratio, Median (Range), %
Whole brain	36 (73.47)	13 (0–286)	1526.8 (1202.8–1793.7)	0.01 (0.00–0.20)
Brain regions				
Frontal	23 (46.94)	0 (0–64)	484.3 (379.6–579.3)	0.00 (0.00–0.47)
Parietal	22 (44.90)	0 (0–35)	184.4 (150.5–224.2)	0.00 (0.00–0.77)
Temporal	29 (59.18)	2 (0–67)	235.4 (186.5–281.6)	0.02 (0.00–1.03)
Limbic	27 (55.10)	1 (0–31)	121.9 (94.8–145.4)	0.02 (0.00–0.70)
Occipital	18 (36.73)	0 (0–31)	149.2 (117.3–177.7)	0.00 (0.00–0.65)
Caudate	16 (32.65)	0 (0–8)	12.4 (7.7–16.3)	0.00 (0.00–2.35)
Putamen	21 (42.86)	0 (0–18)	13.2 (7.9–19.8)	0.00 (0.00–5.30)
Globus pallidum	5 (10.20)	0 (0–8)	6.3 (3.6–8.1)	0.00 (0.00–4.66)
Thalamus	31 (63.27)	2 (0–56)	17.8 (13.7–23.9)	0.46 (0.00–12.35)
Corpus callosum	2 (4.08)	0 (0–1)	6.4 (4.3–8.9)	0.00 (0.00–0.11)
Midbrain	9 (18.37)	0 (0–3)	8.0 (6.0–87.9)	0.00 (0.00–2.99)
Pons	19 (38.78)	0 (0–16)	14.2 (10.8–94.0)	0.00 (0.00–7.79)
Medulla	10 (20.41)	0 (0–9)	5.9 (4.1–85.9)	0.00 (0.00–5.95)
Cerebellum	16 (32.65)	0 (0–23)	150.0 (125.3–183.3)	0.00 (0.00–1.15)

CMB indicates cerebral microbleed.

2018b. Each CMB was first manually localized using a bounding box on the SWI, and the boundary of each CMB within the bounding box was automatically detected using the Canny method,²⁰ followed by the experts' fine-tuning in a voxel-wise manner. Finally, the connected component within the marked boundary was labeled as a CMB. CMB mimics, such as vessels, calcification, partial volumes, air-bone interfaces, and hemorrhage within or adjacent to an infarct, were carefully excluded.^{18,19}

CMB Quantification

To evaluate the topographic distribution of CMBs, whole brain images of each participant were initially parceled into 8 regions, including the lobar (frontal, parietal, temporal, occipital, and limbic regions), sublobar, brainstem, and cerebellum. Whole-brain parcellation was performed with Statistical Parametric Mapping software (<http://www.fil.ion.ucl.ac.uk/spm/>) by spatial normalization of the Montreal Neurological Institute template and Talairach atlas to individual T1-weighted images. The sublobar and brainstem regions were further segmented into subregions using FreeSurfer software (<https://surfer.nmr.mgh.harvard.edu/>). The sublobar region was segmented into caudate, putamen, globus pallidum, thalamus, and corpus callosum; brainstem was segmented into midbrain, pons, and medulla. Finally, the individual's SWI was coregistered to his/her own T1-weighted images, in which the amount and volume of CMBs within each of the 14 brain regions were measured automatically. CMB volume ratio was calculated using total CMB volume in

a specific brain region divided by brain volume of the corresponding region.

Statistical Analysis

Analyses were performed with SPSS software (version 22.0; IBM). We first calculated the percentage of subjects with at least one CMB present in the whole brain, as well as any CMB present in each of the 14 brain regions. CMB count and CMB volume ratio of each participant were also analyzed for the whole brain and each of the 14 brain regions. All data are presented as mean (SD) or median (range) for continuous variables and number (percentage) for discrete variables.

To evaluate the relationship between CMB burdens and disease progression, participants were further divided into 3 groups: *NOTCH3* mutation carriers at preclinical stage (ie, asymptomatic subjects having no stroke or cognitive impairment), symptomatic *NOTCH3* mutation carriers (ie, subjects having stroke or/and cognitive impairment) with disease duration <5 years, and symptomatic *NOTCH3* mutation carriers with disease duration ≥5 years. The CMB count as well as CMB volume ratio were compared among the 3 groups using multivariate linear regression analyses with adjustment of age and sex. The trend *P* was calculated by assuming a dose effect of the 3 groups (ie, mutation carriers at preclinical stage=1, symptomatic carriers with duration <5 years=2, and symptomatic carriers with duration ≥5 years=3) in the regression model. Univariate regression analysis was performed to evaluate the

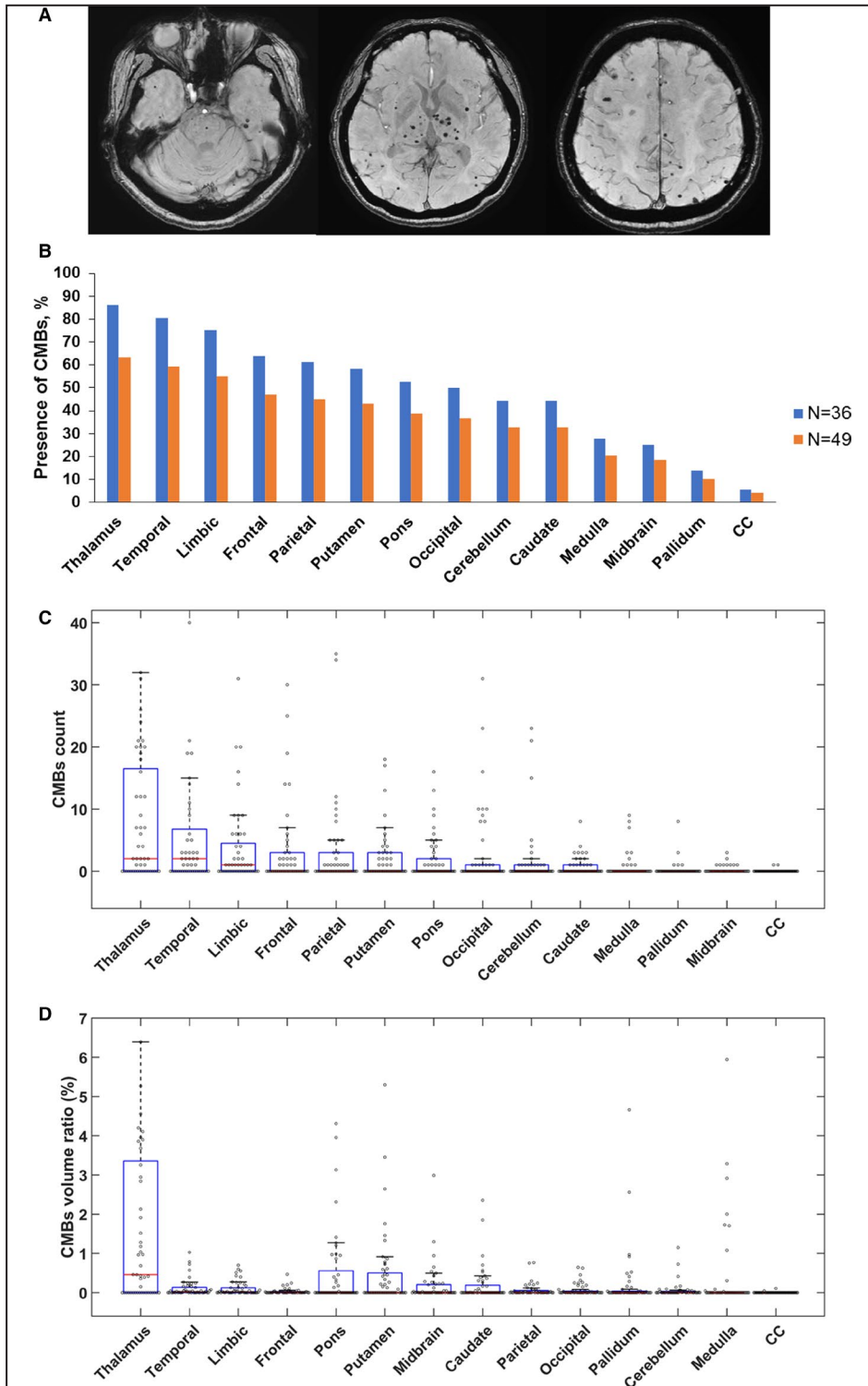


Figure 1. Cerebral microbleed (CMB) burdens in the *NOTCH3* cysteine-altering mutation carriers in the present study.

A, Representative susceptibility-weighted imaging of a 62-year-old woman carrying *NOTCH3* p.R544C mutation with initial presentation of lacunar infarct at the age of 57 years. **B**, Percentage of subjects with CMBs in the 14 brain regions. Orange bar: all study participants in the present study (N=49); blue bar: study participants with at least 1 CMB in the whole brain (N=36). CMB counts (**C**) and CMB volume ratios (**D**) in the corresponding brain regions in all study participants were illustrated by the box plots with whiskers with maximum 1.5 interquartile range (N=49). CC indicates corpus callosum.

Table 3. Comparison of CMB Burdens Among Different Disease Stages

Variable	Mutation Carriers at Preclinical Stage (n=10)	Symptomatic Carriers With Duration <5 y (n=22)	Symptomatic Carriers With Duration ≥5 y (n=17)	Fisher Exact Test or ANOVA
Age, y	53.0 (39.0–77.0)	65.5 (36.0–78.0)	63.0 (41.0–77.0)	<i>P</i> =0.379
Men	2 (20.0)	15 (68.2)	11 (64.7)	<i>P</i> =0.039
Hypertension	2 (20.0)	10 (45.5)	11 (64.7)	<i>P</i> =0.084
Diabetes mellitus	1 (10.0)	3 (13.6)	2 (11.8)	<i>P</i> =1.000
Dyslipidemia	2 (20.0)	8 (36.4)	8 (47.1)	<i>P</i> =0.376
Cigarette smoking	1 (10.0)	9 (40.9)	5 (29.4)	<i>P</i> =0.246
Presence of CMBs	4 (40.0)	17 (77.3)	15 (88.2)	<i>P</i> =0.028
Overall CMB counts	0 (0–8)	15 (0–203)	43 (0–286)	* <i>P</i> trend=0.009
Overall CMB volume ratios, %	0.00 (0.00–0.01)	0.01 (0.00–0.16)	0.03 (0.00–0.20)	* <i>P</i> trend=0.004

Data are given as number (percentage) or median (range). CMB indicates cerebral microbleed. **P* trend was obtained from multivariate linear regression with adjustment of age, sex, and hypertension.

individual effect of cardiovascular risk factors (ie, age, hypertension, diabetes mellitus, hyperlipidemia, and smoking) on total count and volume ratio of CMBs in the whole brain. The associations between CMB burdens (ie, CMB count and CMB volume ratio) and cognitive function (ie, MMSE score) were tested using multivariate linear regression analyses with adjustment of age, sex, and education years. Each 1 of the 14 brain regions was included in the regression model separately to test whether certain brain regions have a regionally specific effect on cognitive performance.

Linear mixed models were used to test whether the severity of CMB burdens (ie, CMB count and CMB volume ratio) varied across the 14 brain regions. The regression model controlled for the within-subject nature of the 14 brain regions by setting up brain regions as a random effect with random intercept, and assuming a compound symmetry structure and restricted maximum likelihood estimation. Later, disease stages were included in the linear mixed models as a fixed, between-subjects factor to test the interaction effect between brain regions and disease stages on CMB burdens.

Table 4. CMB Counts and CMB Volume Ratios in 14 Brain Regions

Brain Regions	CMB Count, Median (Range)			CMB Volume Ratio, Median (Range), %		
	Preclinical Stage (n=10)	Duration <5 y (n=22)	Duration ≥5 y (n=17)	Preclinical Stage (n=10)	Duration <5 y (n=22)	Duration ≥5 y (n=17)
Frontal*	0 (0–0)	0.5 (0–25)	2 (0–64)	0.00 (0.00–0.00)	0.00 (0.00–0.19)	0.02 (0.00–0.47)
Parietal	0 (0–0)	0.5 (0–12)	1 (0–35)	0.00 (0.00–0.00)	0.01 (0.00–0.30)	0.03 (0.00–0.77)
Temporal*	0 (0–1)	2 (0–46)	5 (0–67)	0.00 (0.00–0.01)	0.03 (0.00–0.72)	0.08 (0.00–1.03)
Limbic	0 (0–1)	1 (0–20)	2 (0–31)	0.00 (0.00–0.02)	0.03 (0.00–0.56)	0.06 (0.00–0.70)
Occipital	0 (0–1)	0 (0–23)	1 (0–31)	0.00 (0.00–0.02)	0.00 (0.00–0.65)	0.02 (0.00–0.63)
Caudate	0 (0–0)	0 (0–8)	1 (0–4)	0.00 (0.00–0.00)	0.00 (0.00–1.85)	0.05 (0.00–2.35)
Putamen	0 (0–2)	0 (0–17)	1 (0–18)	0.00 (0.00–0.73)	0.00 (0.00–3.45)	0.21 (0.00–5.30)
Globus pallidum	0 (0–0)	0 (0–8)	0 (0–3)	0.00 (0.00–0.00)	0.00 (0.00–4.66)	0.01 (0.00–2.56)
Thalamus*†	0 (0–2)	2 (0–32)	12 (0–56)	0.00 (0.00–1.04)	0.44 (0.00–6.39)	1.91 (0.00–12.35)
Corpus callosum	0 (0–0)	0 (0–0)	0 (0–1)	0.00 (0.00–0.00)	0.00 (0.00–0.00)	0.00 (0.00–0.11)
Midbrain	0 (0–0)	0 (0–2)	0 (0–3)	0.00 (0.00–0.01)	0.00 (0.00–1.30)	0.02 (0.00–2.99)
Pons	0 (0–0)	0 (0–13)	2 (0–16)	0.00 (0.00–0.00)	0.00 (0.00–4.31)	0.46 (0.00–7.79)
Medulla	0 (0–0)	0 (0–7)	0 (0–9)	0.00 (0.00–0.00)	0.00 (0.00–3.28)	0.00 (0.00–5.95)
Cerebellum	0 (0–2)	0 (0–21)	0 (0–23)	0.00 (0.00–0.02)	0.00 (0.00–0.72)	0.01 (0.00–1.15)

CMB indicates cerebral microbleed.

*CMB counts in the frontal lobe, temporal lobe, and thalamus increased more rapidly as disease advanced, with a significant interaction effect between CMB counts and disease stages in the linear mixed models (*P*<0.05).

†CMB volume ratio in the thalamus increased more rapidly as disease advanced, with a significant interaction effect between CMB volume ratio and disease stages in the linear mixed models (*P*<0.05).

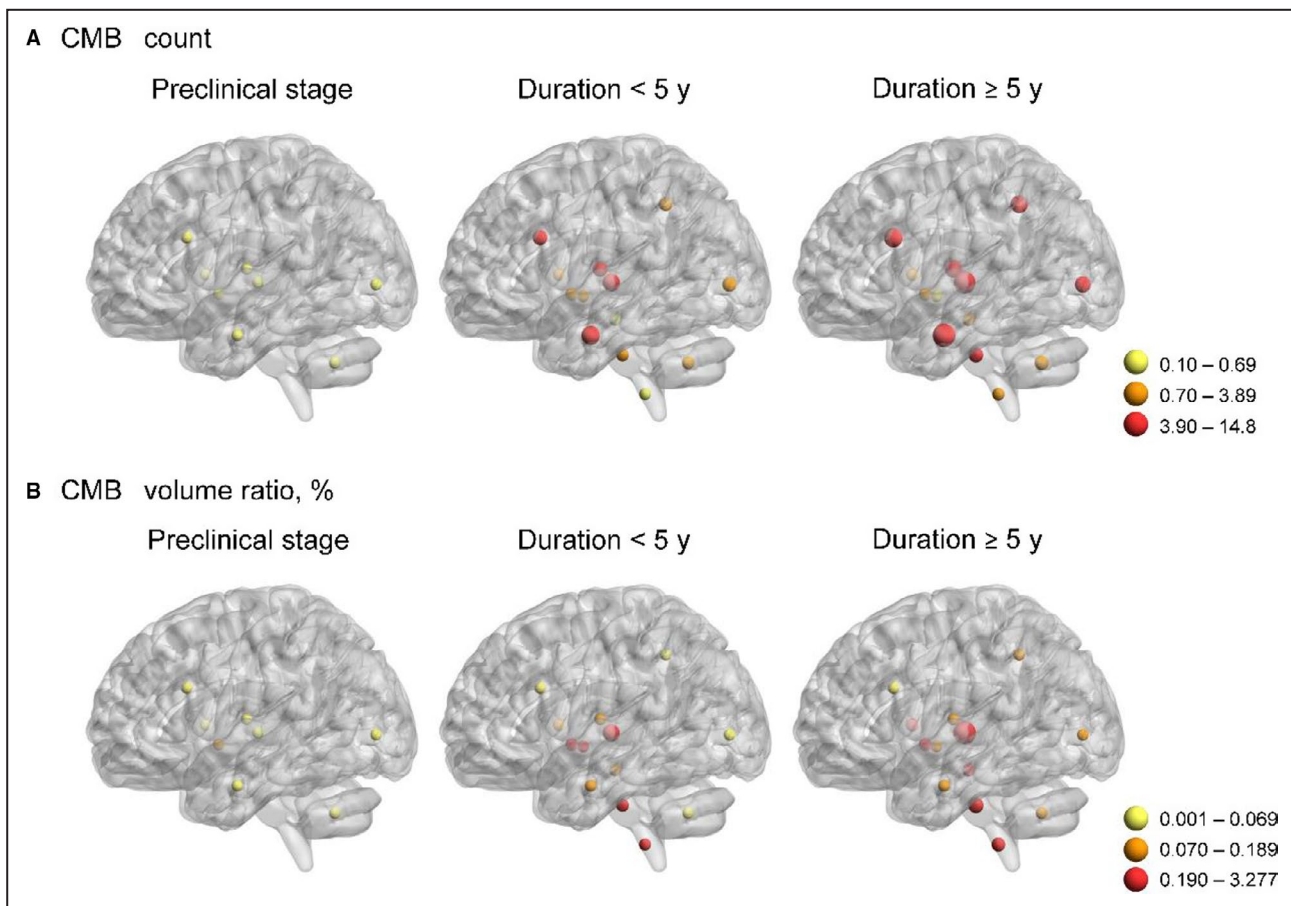


Figure 2. Cerebral microbleed (CMB) burdens in the *NOTCH3* cysteine-altering mutation carriers at different disease stages.

A, Yellow dots represent regions with average CMB count of 0.10 to 0.69. Orange dots represent regions with average CMB count of 0.70 to 3.89. Red dots represent regions with average CMB count of 3.90 to 14.8. **B**, Yellow dots represent regions with average CMB volume ratio of 0.001% to 0.069%. Orange dots represent regions with average CMB volume ratio of 0.070% to 0.189%. Red dots represent regions with average CMB volume ratio of 0.19% to 3.28%.

RESULTS

Demographic information of the study participants is shown in Table 1. *NOTCH3* p.R544C mutation was the most common mutation and was found in 41 of the 49 study participants (83.7%). *NOTCH3* p.S118C mutation was found in 3 people, p.R133C mutation was found in 2 people, and p.R141C, p.R427C, and p.C977S mutations were found in 1 individual each.

Among the 49 participants, 36 (73.5%) had at least 1 CMB detected in the whole brain. CMBs were most commonly present in the thalamus, and 63.3% (31/49) of the participants had CMBs in this brain region (Table 2). CMBs were also frequently detected in the temporal lobe (59.2%), followed by limbic region (55.1%), frontal lobe (46.9%), parietal lobe (44.9%), putamen (42.9%), pons (38.8%), occipital lobe (36.7%), cerebellum (32.7%), and caudate nucleus (32.7%) (Figure 1A and 1B and Table 2). The range of CMB amounts was wide for 13 individuals having 0 CMBs

and 1 having a maximum of 286 CMBs in the whole brain. The CMBs were most abundant in the thalamus, followed by temporal lobe (Figure 1C and Table 2). When the brain volume of each region was taken into account, the density of CMBs was highest in the thalamus, with a median CMB volume ratio of 0.46%, and then in the temporal and limbic lobes (Figure 1D and Table 2).

We then analyzed the individual effect of cardiovascular risk factors (ie, age, hypertension, diabetes mellitus, hyperlipidemia, and smoking) on global CMB burdens. Presence of hypertension was found to be significantly associated with CMB counts in the whole brain ($\beta=64.4$; 95% CI, 32.4–96.9; $P<0.001$), as well as CMB volume ratio in the whole brain ($\beta=0.05$; 95% CI, 0.02–0.07; $P<0.001$). None of the other cardiovascular risk factors, including age, sex, diabetes mellitus, hyperlipidemia, and smoking habit, was related to global CMB burdens in the univariate regression analysis.

Table 5. Associations Between CMB Burdens in Different Brain Regions and Mini-Mental State Examination Scores

Brain Region	CMB Count		CMB Volume Ratio, %	
	β (95% CI)	P Value*	β (95% CI)	P Value*
Whole brain	-0.05 (-0.07 to -0.02)	1.0×10 ^{-3†}	-58.86 (-93.83 to -23.89)	1.5×10 ^{-3†}
Frontal	-0.31 (-0.46 to -0.16)	1.2×10 ^{-4†}	-41.25 (-60.67 to -21.84)	9.9×10 ^{-5†}
Parietal	-0.34 (-0.58 to -0.11)	0.005	-15.29 (-25.83 to -4.75)	0.005
Temporal	-0.19 (-0.32 to -0.07)	3.1×10 ^{-3†}	-12.79 (-20.46 to -5.12)	1.6×10 ^{-3†}
Limbic	-0.26 (-0.54 to 0.02)	0.070	-10.63 (-20.53 to -0.74)	0.036
Occipital	-0.32 (-0.61 to -0.40)	0.026	-15.72 (-27.12 to -4.31)	0.008
Caudate	-0.83 (-2.09 to 0.43)	0.192	-3.22 (-7.17 to -0.74)	0.108
Putamen	-0.42 (-0.85 to 0.01)	0.058	-1.53 (-3.35 to 0.29)	0.098
Globus pallidum	-0.78 (-2.29 to 0.73)	0.304	-1.79 (-4.19 to 0.61)	0.139
Thalamus	-0.16 (-0.31 to -0.00)	0.046	-0.60 (-1.25 to 0.04)	0.066
Corpus callosum	1.14 (-8.22 to 10.50)	0.808	11.42 (-102.72 to 125.55)	0.841
Midbrain	-1.62 (-4.71 to 1.47)	0.295	-3.08 (-6.83 to 0.67)	0.105
Pons	-0.97 (-1.42 to -0.52)	7.5×10 ^{-5†}	-2.61 (-3.67 to -1.56)	9.8×10 ^{-6†}
Medulla	-1.07 (-1.99 to -0.14)	0.025	-1.89 (-3.56 to -0.22)	0.028
Cerebellum	-0.38 (-0.77 to 0.01)	0.056	-10.12 (-19.36 to -0.87)	0.033

CMB indicates cerebral microbleed.

*P value was obtained from multivariate linear regression with adjustment of age, sex, and education years.

†To eliminate the concern of multiple testing, a 2-sided P<0.00357 (0.05/14) was considered statistically significant.

When the study participants were divided into 3 groups according to the disease duration, there was a significant trend for subjects with a longer disease duration having more CMBs in the whole brain (Table 3). The medians (ranges) of CMB counts in the whole brain were 0 (0–8), 15 (0–203), and 43 (0–286) for participants at the preclinical stage, those with disease duration <5 years, and those with disease duration ≥5 years, respectively. In addition, CMB volume ratios in the whole brain were also significantly associated with disease duration. After adjusting for age, sex, and hypertension, disease duration remained to be an independent predictor for CMB burdens in the multivariate regression analysis (P trend=0.009 and 0.004 for CMB counts and CMB volume ratios, respectively).

We then compared CMB burdens across the 14 brain regions using repeated measures regression (Table 4). In the overall participants, CMB counts were significantly different among the brain regions (F[2.28, 109.35]=11.18; P<0.001). Also, CMB volume ratios in the 14 brain regions varied (F[1.75, 83.86]=17.12; P<0.001). We further included disease stages in the linear mixed models to test whether CMB burdens in any brain region increased more rapidly than other regions as the disease progressed. We found a significant interaction effect between brain regions and disease stages on CMB burdens. The increments of CMB counts in the thalamus (β=5.83; SE=1.44; P<0.001), in the temporal lobe (β=4.65; SE=1.44; P=0.001), and in the frontal lobe (β=3.31; SE=1.44; P=0.022) were significantly

higher than those in other brain regions as disease advanced. In addition, CMB volume ratios in the thalamus increased more rapidly than other brain regions as disease progressed (β=1.19; SE=0.23; P<0.001). Figure 2 demonstrates the CMB burdens in the 14 brain regions for NOTCH3 mutation carriers at different disease stages. As the disease progressed from preclinical stage to an advanced stage, the CMB burdens grew gradually in each brain region with increasing CMB counts and CMB volume ratio (Figure 2A and 2B).

We then tested whether there was a significant correlation between CMB burdens and the global cognitive function in NOTCH3 mutation carriers. After adjusting for age, sex, and education years, a greater CMB count and a higher CMB volume ratio in the whole brain were significantly associated with decreased MMSE scores (P=1.0×10⁻³ and 1.5×10⁻³, respectively) (Table 5). In addition, both the CMB count and CMB volume ratio in the frontal lobe, temporal lobe, and pons were significantly associated with cognitive performance in the study participants (Table 5). Although CMBs were most abundant in the thalamus, neither CMB counts nor CMB volume ratio in the thalamus was related to MMSE scores.

DISCUSSION

The present study demonstrates the panorama of CMBs, including the count, volume ratio, and topographic distribution, in a Taiwanese cohort of NOTCH3 cysteine-altering mutation carriers at different disease

stages. The present study has 4 major findings. First, CMBs are common in CADASIL for 73.5% of the overall participants having at least 1 CMB in their brain. The percentages of subjects with CMBs are 40.0%, 77.3%, and 88.2% in mutation carriers at preclinical stage, symptomatic subjects with disease duration <5 years, and those with disease duration \geq 5 years, respectively. Second, thalamus and temporal lobe are the brain regions most frequently having CMBs, as well as the area with the greatest CMB counts among the 14 brain regions. For the density of CMBs, thalamus has the highest CMB volume ratio versus other brain regions. Third, we found a significant association between CMB burdens and disease severity, which was modeled by disease duration and cognitive function. This finding supports CMBs as a potential maker to monitor disease severity in CADASIL. Last, CMBs located at disparate brain regions may have different clinical influences. In our cohort, CMB counts in the thalamus, frontal lobe, and temporal lobe increased significantly with the duration of the disease, whereas CMB counts in the frontal lobe, temporal lobe, and pons were significantly correlated with cognitive performance. Our results highlight the roles of CMBs as a surrogate marker for disease progression of CADASIL and emphasize the importance of analyzing both the quantity and topographic distributions of CMBs in patients with CADASIL.

The prevalence of CMBs in CADASIL varies across different cohort studies. According to the previous studies in white CADASIL populations, the prevalences of CMBs in a Dutch cohort,² Italian-British cohort,⁶ and Paris-Munich cohort^{8,21} are 25%, 34%, and 35.5%, respectively. For the studies conducted in Asian countries, the prevalence of CMBs appears to be much higher, with CMBs detected in 54.9% to 66% of the Korean CADASIL patients^{7,22} and 87.5% of the Taiwanese CADASIL patients.¹⁷ Ethnicity might be one of the reasons for the discrepancies because Asians are well known for being prone to intracerebral hemorrhage.^{23,24} Other than ethnic difference, our study subjects had an older age at MRI examination and a higher prevalence of hypertension than the study subjects in the white CADASIL studies.^{2,6,8} Age and hypertension are known risk factors of CMBs in CADASIL,^{2,7,21,22} so a higher prevalence and a greater burden of CMBs in our study participants may be caused by discrepancies of these demographic characteristics. In addition, the present study used fine-cut, high-resolution MRI sequences (3-T MRI with SWI) that may improve the sensitivity and accuracy of CMB assessment¹⁸ and, hence, more CMBs were detected.

Consistent with the findings in other CADASIL cohorts,^{2,6-8,21,22} the present study demonstrated a greater burden and widespread distribution of CMBs in CADASIL patients than those reported in the

general elderly population and patients with ischemic stroke.^{9,25-28} Our findings again emphasize that the clinical spectrum of CADASIL not only includes ischemic (eg, WMHs and lacunar infarcts) but also hemorrhagic brain parenchymal insults. More studies are needed to elucidate the pathophysiological characteristics to develop management strategy in CADASIL-related brain hemorrhages. Just like the findings in other CADASIL studies,^{2,6,7,22,29} thalamus is the most common region with CMBs and the area with highest CMB burdens among the 14 brain regions. Lobar (corticosubcortical) regions have been shown to be the second most common area with CMBs in previous studies.^{6,7,22,29} We further segmented the lobar regions and found that CMB counts were significantly higher in the temporal and frontal lobes than other lobar regions. These findings imply that CMBs predominantly presenting in the thalamus and temporofrontal lobe might be a radiologic feature that helps distinguishing CADASIL from other CSVDs, such as cerebral amyloid angiopathy and hypertensive microvasculopathy. Future studies, including head-to-head comparison between CADASIL patients and subjects with other CSVDs, are needed to test this postulation.

CMB burdens in the thalamus had a strong association with disease duration but were not correlated to cognitive performance in our study participants. This phenomenon is probably because of a ceiling effect of CMBs in the thalamus. Among the 14 brain regions, CMB counts in the frontal lobe, temporal lobe, and pons were most correlated with MMSE scores in the present study. These topographic characteristics of CMBs might provide clues to the pathomechanisms responsible for cognitive decline in CADASIL. Among the many cognitive domains that are progressively deteriorated in the disease course of CADASIL, executive function and processing speed are most profoundly affected.^{30,31} Our findings lend support to the hypothesis that disturbance of the frontal-subcortical circuits is responsible for the executive dysfunction in patients with CSVDs.^{32,33} Furthermore, lesions in pons, in which area frontal-subcortical circuits have projections to, also have been implicated in executive dysfunction.^{34,35}

The present study has advantages and limitations. We sophisticatedly illustrate the anatomical distribution and quantity of CMBs and evaluate their clinical significance in CADASIL. However, this is a cross-sectional study rather than a longitudinal study. We acknowledge that the settlement of disease onset might not be precise and would obscure the estimation of disease duration in the present study. A longitudinal study with a large population is needed to validate the feasibility of using CMBs to monitor disease progression in CADASIL. The other limitation of the present study is

that we did not analyze the effects of WMHs or lacunes on disease severity. Both WMHs and lacunar infarcts may account for low MMSE scores in the absence of CMBs.³⁶ Last, more studies are required before generalizing the current findings to all cysteine-altering mutations and non-Asian populations.

CONCLUSIONS

CMBs may have an influential role in the clinical manifestations of CADASIL. CMB burdens and their distribution in different brain regions may be capable to serve as disease markers for monitoring the progression of CADASIL.

ARTICLE INFORMATION

Received February 17, 2020; accepted May 20, 2020.

Affiliations

From the Department of Neurology, Neurological Institute (C.-P.C., Y.-C. Lee, Y.-C. Liao), Department of Radiology (F.-C.C.), and Integrated Brain Research Laboratory, Department of Medical Research (L.-F.C.), Taipei Veterans General Hospital, Taipei, Taiwan; and School of Medicine (C.-P.C., F.-C.C., Y.-C. Lee, Y.-C. Liao), Institute of Brain Science and Institute of Biomedical Informatics (J.-W.C., W.-C.L., L.-F.C.), and Brain Research Center (C.-P.C., Y.-C. Lee, L.-F.C., Y.-C. Liao), National Yang-Ming University, Taipei, Taiwan.

Sources of Funding

This study was supported by the grants from Ministry of Science and Technology, Taiwan (104-2314-B-075-045-MY4, 107-2221-E-010-013, and 108-2628-B075-005), Taipei Veterans General Hospital (V108C-076), and Brain Research Center, National Yang-Ming University, from The Featured Areas Research Center Program within the framework of the Higher Education Sprout Project by the Ministry of Education in Taiwan.

Disclosures

None.

REFERENCES

- Chabriat H, Joutel A, Dichgans M, Tournier-Lasserre E, Bousser MG. CADASIL. *Lancet Neurol*. 2009;8:643–653.
- Lesnik Oberstein SA, van den Boom R, van Buchem MA, van Houwelingen HC, Bakker E, Vollebregt E, Ferrari MD, Breuning MH, Haan J. Cerebral microbleeds in CADASIL. *Neurology*. 2001;57:1066–1070.
- van den Boom R, Lesnik Oberstein SA, Ferrari MD, Haan J, van Buchem MA. Cerebral autosomal dominant arteriopathy with subcortical infarcts and leukoencephalopathy: MR imaging findings at different ages—3rd–6th decades. *Radiology*. 2003;229:683–690.
- Viswanathan A, Gschwendtner A, Guichard JP, Buffon F, Cumurciuc R, O'Sullivan M, Holtmannspötter M, Pachai C, Bousser MG, Dichgans M, et al. Lacunar lesions are independently associated with disability and cognitive impairment in CADASIL. *Neurology*. 2007;69:172–179.
- Liem MK, Lesnik Oberstein SA, Haan J, van der Neut IL, Ferrari MD, van Buchem MA, Middelkoop HA, van der Grond J. MRI correlates of cognitive decline in CADASIL: a 7-year follow-up study. *Neurology*. 2009;72:143–148.
- Nannucci S, Rinnoci V, Pracucci G, MacKinnon AD, Pescini F, Adib-Samii P, Bianchi S, Dotti MT, Federico A, Inzitari D, et al. Location, number and factors associated with cerebral microbleeds in an Italian-British cohort of CADASIL patients. *PLoS One*. 2018;13:e0190878.
- Lee JS, Ko K, Oh JH, Park JH, Lee HK, Florioli D, Paganini-Hill A, Fisher M. Cerebral microbleeds, hypertension, and intracerebral hemorrhage in cerebral autosomal-dominant arteriopathy with subcortical infarcts and leukoencephalopathy. *Front Neurol*. 2017;8:203.
- Puy L, De Guio F, Godin O, Duering M, Dichgans M, Chabriat H, Jouvent E. Cerebral microbleeds and the risk of incident ischemic stroke in CADASIL (Cerebral Autosomal Dominant Arteriopathy With Subcortical Infarcts and Leukoencephalopathy). *Stroke*. 2017;48:2699–2703.
- Poels MM, Vernooij MW, Ikram MA, Hofman A, Krestin GP, van der Lugt A, Breteler MM. Prevalence and risk factors of cerebral microbleeds: an update of the Rotterdam scan study. *Stroke*. 2010;41:S103–S106.
- Park JH, Seo SW, Kim C, Kim GH, Noh HJ, Kim ST, Kwak KC, Yoon U, Lee JM, Lee JW, et al. Pathogenesis of cerebral microbleeds: in vivo imaging of amyloid and subcortical ischemic small vessel disease in 226 individuals with cognitive impairment. *Ann Neurol*. 2013;73:584–593.
- Tsai HH, Tsai LK, Chen YF, Tang SC, Lee BC, Yen RF, Jeng JS. Correlation of cerebral microbleed distribution to amyloid burden in patients with primary intracerebral hemorrhage. *Sci Rep*. 2017;7:44715.
- Fazekas F, Barkhof F, Wahlund LO, Pantoni L, Erkinjuntti T, Scheltens P, Schmidt R. CT and MRI rating of white matter lesions. *Cerebrovasc Dis*. 2002;13:31–36.
- Folstein MF, Folstein SE, McHugh PR. "Mini-mental state": a practical method for grading the cognitive state of patients for the clinician. *J Psychiatr Res*. 1975;12:129–138.
- Jones DW, Hall JE. Seventh report of the Joint National Committee on prevention, detection, evaluation, and treatment of high blood pressure and evidence from new hypertension trials. *Hypertension*. 2004;43:1–3.
- American Diabetes Association. Diagnosis and classification of diabetes mellitus. *Diabetes Care*. 2014;37:S81–S90.
- National Cholesterol Education Program (NCEP) expert panel on detection, evaluation, and treatment of high blood cholesterol in adults (Adult Treatment Panel III): third report of the National Cholesterol Education Program (NCEP) expert panel on detection, evaluation, and treatment of high blood cholesterol in adults (Adult Treatment Panel III) final report. *Circulation*. 2002;106:3143–3421.
- Liao YC, Hsiao CT, Fuh JL, Chern CM, Lee WJ, Guo YC, Wang SJ, Lee IH, Liu YT, Wang YF, et al. Characterization of CADASIL among the Han Chinese in Taiwan: distinct genotypic and phenotypic profiles. *PLoS One*. 2015;10:e0136501.
- Greenberg SM, Vernooij MW, Cordonnier C, Viswanathan A, Al-Shahi Salman R, Warach S, Launer LJ, Van Buchem MA, Breteler MM. Cerebral microbleeds: a guide to detection and interpretation. *Lancet Neurol*. 2009;8:165–174.
- Gregoire SM, Chaudhary UJ, Brown MM, Yousry TA, Kallis C, Jäger HR, Werring DJ. The Microbleed Anatomical Rating Scale (MARS): reliability of a tool to map brain microbleeds. *Neurology*. 2009;73:1759–1766.
- Canny J. A computational approach to edge detection. *IEEE Trans Pattern Anal Mach Intell*. 1986;8:679–698.
- Viswanathan A, Guichard JP, Gschwendtner A, Buffon F, Cumurciuc R, Boutron C, Vicaut E, Holtmannspötter M, Pachai C, Bousser MG, et al. Blood pressure and haemoglobin A1c are associated with microhaemorrhage in CADASIL: a two-centre cohort study. *Brain*. 2006;129:2375–2383.
- Lee JS, Kang CH, Park SQ, Choi HA, Sim KB. Clinical significance of cerebral microbleeds locations in CADASIL with R544C NOTCH3 mutation. *PLoS One*. 2015;10:e0118163.
- An SJ, Kim TJ, Yoon BW. Epidemiology, risk factors, and clinical features of intracerebral hemorrhage: an update. *J Stroke*. 2017;19:3–10.
- Mehta RH, Cox M, Smith EE, Xian Y, Bhatt DL, Fonarow GC, Peterson ED. Race/ethnic differences in the risk of hemorrhagic complications among patients with ischemic stroke receiving thrombolytic therapy. *Stroke*. 2014;45:2263–2269.
- Cordonnier C, Al-Shahi Salman R, Wardlaw J. Spontaneous brain microbleeds: systematic review, subgroup analyses and standards for study design and reporting. *Brain*. 2007;130:1988–2003.
- Werring DJ, Coward LJ, Losseff NA, Jäger HR, Brown MM. Cerebral microbleeds are common in ischemic stroke but rare in TIA. *Neurology*. 2005;65:1914–1918.
- Graff-Radford J, Botha H, Rabinstein AA, Gunter JL, Przybelski SA, Lesnick T, Huston J III, Flemming KD, Preboske GM, Senjem ML, et al. Cerebral microbleeds: prevalence and relationship to amyloid burden. *Neurology*. 2019;92:e253–e262.
- Wang PN, Chou KH, Peng LN, Liu LK, Lee WJ, Chen LK, Lin CP, Chung CP. Strictly lobar cerebral microbleeds are associated with increased white matter volume. *Transl Stroke Res*. 2020;11:29–38.
- Wollenweber FA, Baykara E, Zedde M, Gesierich B, Achmüller M, Jouvent E, Viswanathan A, Ropele S, Chabriat H, Schmidt R, et al. Cortical superficial siderosis in different types of cerebral small vessel disease. *Stroke*. 2017;48:1404–1407.

-
30. Amberla K, Wäljas M, Tuominen S, Almkvist O, Pöyhönen M, Tuisku S, Kalimo H, Viitanen M. Insidious cognitive decline in CADASIL. *Stroke*. 2004;35:1598–1602.
 31. Dichgans M. Cognition in CADASIL. *Stroke*. 2009;40:S45–S47.
 32. O’Sullivan M, Barrick TR, Morris RG, Clark CA, Markus HS. Damage within a network of white matter regions underlies executive dysfunction in CADASIL. *Neurology*. 2005;65:1584–1590.
 33. Duering M, Zieren N, Hervé D, Jouvent E, Reyes S, Peters N, Pachai C, Opherk C, Chabriat H, Dichgans M. Strategic role of frontal white matter tracts in vascular cognitive impairment: a voxel-based lesion-symptom mapping study in CADASIL. *Brain*. 2011;134:2366–2375.
 34. Vataja R, Pohjasvaara T, Mäntylä R, Ylikoski R, Leppävuori A, Leskelä M, Kalska H, Hietanen M, Aronen HJ, Salonen O, et al. MRI correlates of executive dysfunction in patients with ischaemic stroke. *Eur J Neurol*. 2003;10:625–631.
 35. Omar R, Warren JD, Ron MA, Lees AJ, Rossor MN, Kartsounis LD. The neuro-behavioural syndrome of brainstem disease. *Neurocase*. 2007;13:452–465.
 36. Jokinen H, Koikkalainen J, Laakso HM, Melkas S, Nieminen T, Brander A, Korvenoja A, Rueckert D, Barkhof F, Scheltens P, et al. Global burden of small vessel disease-related brain changes on MRI predicts cognitive and functional decline. *Stroke*. 2020;51:170–178.